

# A comparison of the SAO-Hipparcos reference frames

E.F. Arias\*, R.G. Cionco, R.B. Orellana\*, and H. Vucetich\*

Facultad de Ciencias Astronómicas y Geofísicas (FCAG), Paseo del Bosque S/N, Universidad Nacional de La Plata, 1900, Argentina

Received 6 December 1999 / Accepted 10 May 2000

**Abstract.** The reference systems defined by the SAO and Hipparcos catalogues are compared using vector spherical harmonic analysis. The differences between astrometric data in both catalogues have been grouped into different data sets and separate harmonic analysis performed on them. The Fourier coefficients yield estimates of systematic errors in SAO catalogue.

**Key words:** astrometry – reference systems – catalogs

## 1. Introduction

The Smithsonian Astrophysical Observatory Star Catalogue (SAO) has been largely used as the reference catalogue in the reduction of astrometric plates in the past. These plates contain relevant information on comet and asteroid positions and motions.

The International Celestial Reference System (ICRS) is nowadays the conventional IAU Celestial System, materialized primarily by the International Celestial Reference Frame (ICRF). The optical realization of the ICRS is the Hipparcos Star Catalogue. The IAU recommended to perform all necessary ties between frames of different nature serving to various purposes, and the present realizations of the ICRS.

We compared the coordinate and proper motion differences between more than 100000 stars common to SAO and Hipparcos catalogues using vector spherical harmonic analysis. The results reveal distortions in the sphere defined through the SAO star positions, the most important effects being in declination, associated to a large displacement field towards the South pole. The coefficients of the series which represent the differences provide the tool to transform positions reduced with the SAO catalogue into the ICRS.

## 2. The International Celestial Reference System (ICRS)

The celestial reference system of the International Earth Rotation Service (IERS, Arias et al. 1995) was adopted since January 1998 by the International Astronomical Union (IAU) as the conventional celestial reference system under the name International Celestial Reference System (ICRS). The ICRS follows

the IAU recommendations (Bergeron 1992) on the definition of the system. The origin of the system is at the barycentre of the Solar System; the principal plane is close to the mean equator at J2000.0. The shift of the Earth's mean pole at J2000.0 relative to the ICRS celestial pole is  $18.0 \pm 0.1$  mas in the direction 12h and  $5.3 \pm 0.1$  mas in the direction 18h. As required by the IAU, and for the sake of continuity with the previous conventional system, the direction of the ICRS pole is consistent with that of the FK5 system within the uncertainty of the latter; assuming that the error in the precession rate is absorbed by the proper motions of stars, the uncertainty of the FK5 pole position relative to the mean pole at J2000.0 is  $\pm 50$  mas. The IAU recommended that the origin of right ascensions of the new celestial reference system be close to the dynamical equinox at J2000.0. The location of the dynamical equinox in the ICRS was determined within  $\pm 10$  mas by Folkner et al. (Folkner et al. 1994); they conclude that the x-axis of the ICRS is offset from the mean equinox at epoch J2000.0 by  $78 \pm 10$  mas.

## 3. The International Celestial Reference Frame (ICRF)

The ICRS is materialized by the precise coordinates of extragalactic radio sources observed with the technique of Very Long Baseline Interferometry (VLBI). The previous realizations of the conventional celestial reference system assumed that the coordinates of the objects were conventional, i.e., their numerical values remained fixed for some time. This is the philosophy adopted in the series of FK catalogues; when a new catalogue was released, the reference system implied in it changed its orientation relative to the previous one. In the case of the ICRS, the axes of the system are considered conventionally fixed to those of the initial realization; source coordinates are susceptible to change if justified by their improvement. As the system should not change with the different realizations, a process of maintenance is applied. The ICRS maintenance implies a permanent monitoring of sources in ICRS to study their positional stability, the improvement of the models adopted and the control of the invariability of the directions of its axes.

The first realization of the ICRF (Ma et al. 1997, 1998) is based on radio positions obtained in a general solution for all dual frequency Mark III VLBI data available through the middle of 1995. The quasi-inertial reference system is defined by the mean J2000.0 coordinates of 212 high-astrometric-quality radio sources; their positional accuracy is better than about 1 mas both

---

Send offprint requests to: R.B. Orellana  
(rorellana@fcaglp.fcaglp.unlp.edu.ar)

\* Member of CONICET

in right ascension and declination. Additional 396 objects that either need further observation to conclude about their quality, or being unsuitable to define an accurate reference frame, serve to link ICRF to other frames. The maintenance of the axes is assured by the 212 defining sources of the frame.

#### 4. Accessibility of ICRS

The direct access to the extragalactic objects is most precise through VLBI observations; most sources are too faint to be successfully observed with optical instruments. Therefore, the ICRS is not widely available to all users, except if it is tied to other major reference frames. The IAU decided that the Hipparcos stellar reference frame be the realization of the ICRS in optical wavelengths (Kovalevsky et al. 1997). Furthermore, the IAU has decided that the International Earth Rotation Service and the IAU Working Group on reference frames, should assure the ties between ICRF and reference frames at others wavelengths (Andersen 1999).

#### 5. The Hipparcos Catalogue

As a result of the Hipparcos mission two astrometric catalogues were produced, the Hipparcos Catalogue, containing about 120000 stars, and the Tycho Catalogue with more than one million stars. The stellar coordinates were obtained from observations conducted by the satellite in the period 1989.85–1993.21; the epoch of Hipparcos catalogue is J1991.25. The stellar Hipparcos coordinates represent the International Celestial Reference System (ICRS) within  $\pm 0.6$  mas for the three axes; the residual rotations of the Hipparcos frame with respect to the ICRF are at level of  $\pm 0.25$  mas/yr also for the three axes (ESA 1997). The IAU adopted Hipparcos Stellar Catalogue as the realization of the ICRS in optical wavelengths.

The basic astrometric data in Hipparcos Catalogue includes positions, proper motions and trigonometric parallaxes of 118218 stars. For visual magnitudes up to 9 the median astrometric precision for single stars at the epoch of the catalogue is 0.77 mas for the right ascensions and 0.64 mas for the declinations, 0.88 and 0.74 mas/yr for the proper motions in right ascension and declination respectively. The density of the catalogue is of three stars per square degree with a limiting magnitude of 12.4.

It is to be noted that Hipparcos Catalogue (1997) has not been tied to the FK5 system, but only to the ICRS. Considering that this latter is coincident with the FK5 within its uncertainties (Arias et al. 1995), Hipparcos frame can be regarded as representing the J2000 (FK5) system but without its regional errors (Mignard & Froeschlé 2000).

#### 6. The SAO Catalogue

The Smithsonian Astrophysical Observatory Star Catalogue (SAO 1966) results from the combination of several earlier catalogs: the FK4, FK3, GC, AGK2, AGK1, Greenwich AC, Yale, Cape, Cape Zone, Me3 and Me4. The new compilation gives

positions and proper motion for 258997 stars, having an average distribution of 6 stars per square degree. The star positions have an average standard deviation of  $0.2''$  at their original epochs ( $0.5''$  at epoch 1963.5). The equinox is 1950.0 and the system that of the FK4.

The 1984 version of the SAO contains the corrected and extended cross identifications, all errata published up to January 1984. Clayton A. Smith of the U.S. Naval Observatory, provided positions and proper motions at equinox and epoch J2000.0 and on the system of the FK5. These data have been added to the 1990 version of the machine-readable SAO Catalog (Roman & Warren 1990)

#### 7. The basic data set

A set of 101352 stars with SAO reference and astrometric solution were selected from the Hipparcos catalogue (ESA 1997). Position  $(\alpha, \delta)$  and proper motion parameters  $(\mu_\alpha \cos \delta, \mu_\delta)$  were read, together with the corresponding error matrices.

The data was transformed from the Hipparcos epoch (J1991.25) to J2000 and the corresponding error matrices were computed assuming a linear motion model:

$$\alpha_{2000.0} = \alpha_{1991.25} + \mu_\alpha \cos \delta \frac{(T - T_0)}{\cos \delta} \quad (1)$$

$$\begin{aligned} \sigma_{\alpha \cos \delta_{2000.0}}^2 &= \sigma_{\alpha \cos \delta_{1991.25}}^2 + \sigma_{\mu_\alpha \cos \delta}^2 (T - T_0)^2 \\ &+ 2\rho_{\alpha \cos \delta}^{\mu_\alpha \cos \delta} \sigma_{\alpha \cos \delta} \sigma_{\mu_\alpha \cos \delta} (T - T_0) \end{aligned} \quad (2)$$

and similar equations for the declination components. In these equations,  $T_0$  is the initial epoch,  $T$  the final epoch,  $\sigma$  and  $\rho$  the standard deviations and correlation coefficients among position and proper motion parameters. Data for the same star set was read from the SAO catalogue (SAO 1966) and the error matrices were computed for J2000 using a linear motion model. Finally, the differences and the respective standard deviations were computed for each of the astrometric parameters. Four stars with gross differences in the position were eliminated, so the final data set consisted in 101348 stars. Each entry in the data set consisted in the following fields:

1. IN-HIPP: The identification number in the Hipparcos catalogue.
2. IN-SAO: The identification number in the SAO catalogue.
3.  $\alpha$ : Hipparcos Right ascension
4.  $\delta$ : Hipparcos declination
5.  $\Delta\alpha \cos \delta$ : SAO-HIPP differences in  $\alpha \cos \delta$  [mas].
6.  $\Delta\delta$ : SAO-HIPP differences in  $\delta$ . [mas]
7.  $\sigma_{\Delta\alpha \cos \delta}$ : Standard deviation of parameter 5. [mas]
8.  $\sigma_{\Delta\delta}$ : Standard deviation of parameter 6. [mas]
9.  $\mu_\alpha \cos \delta$ :  $\alpha$  component of proper motion [mas/yr].
10.  $\mu_\delta$ :  $\delta$  component of proper motion [mas/yr].
11.  $\Delta\mu_\alpha \cos \delta \equiv \Delta\mu_\alpha$ : SAO-HIPP differences in proper motion,  $\alpha$  component [mas/yr].
12.  $\Delta\mu_\delta$ : SAO-HIPP differences in proper motion,  $\delta$  component [mas/yr].

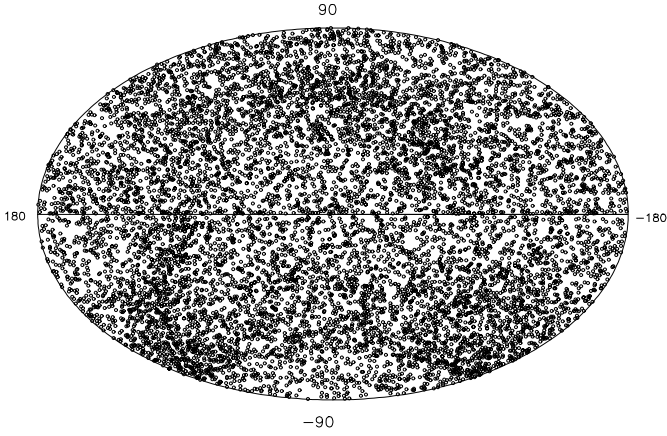


**Fig. 1.** Distribution of stars in the G1 group. The origin of the right ascensions is at the center. The distribution of the other groups is similar to this one

**Table 1.** Initial statistics of the data set. The units for the second column is arcsec, for all the others, milliarcsec.  $\langle \Delta\alpha \rangle$  is an abbreviation for  $\langle \Delta\alpha \cos \delta \rangle$ , and the same for  $\langle \Delta\mu_\alpha \rangle$ .

| Gr. | RMS   | Position                       |                                | Proper motion |                                    |                                    |
|-----|-------|--------------------------------|--------------------------------|---------------|------------------------------------|------------------------------------|
| Id. |       | $\langle \Delta\alpha \rangle$ | $\langle \Delta\delta \rangle$ | RMS           | $\langle \Delta\mu_\alpha \rangle$ | $\langle \Delta\mu_\delta \rangle$ |
| G1  | 1.82  | -75.15                         | -79.77                         | 22.49         | -0.24                              | -0.91                              |
| G2  | 1.84  | -101.29                        | -91.36                         | 22.84         | -0.57                              | -1.01                              |
| G3  | 1.92  | -125.75                        | -67.73                         | 23.72         | -0.72                              | -0.80                              |
| G4  | 1.89  | -92.16                         | -85.61                         | 23.26         | -0.39                              | -0.97                              |
| G5  | 1.84  | -97.62                         | -105.27                        | 22.58         | -0.42                              | -1.31                              |
| G6  | 1.97  | -96.21                         | -94.42                         | 22.82         | -0.33                              | -1.11                              |
| G7  | 1.90  | -100.35                        | -85.52                         | 22.59         | -0.35                              | -0.91                              |
| G8  | 1.94  | -106.82                        | -79.59                         | 24.45         | -0.62                              | -1.04                              |
| G9  | 1.86  | -105.13                        | -92.77                         | 22.79         | -0.50                              | -1.06                              |
| G10 | 1.89  | -81.93                         | -95.95                         | 21.81         | -0.31                              | -1.20                              |
| All | 16.27 | -101.28                        | -81.22                         | 22.96         | -0.44                              | -1.03                              |

13.  $\sigma_{\Delta\mu_\alpha \cos \delta} \equiv \sigma_{\Delta\mu_\alpha}$ : Standard deviation of parameter 11. [mas/yr]  
 14.  $\sigma_{\Delta\mu_\delta}$ : Standard deviation of parameter 12. [mas/yr]

Due to the large number of items, the data was divided in 10 subsets, covering the full sky. Each subset was formed taking the stars whose index end in the digits 0–9, i.e. the first subset contains all stars whose numbers end by 0, the second subset contains all stars whose numbers end by 1, and so on. Table 1 shows the initial statistics for full data set and the 10 subsets. Fig. 1 shows the covering of the sky by the G1 group of stars. The difference position errors histogram is shown in Fig. 2. They are obviously dominated by the SAO catalogue errors.

## 8. The adjusted model

The differences in the data set (position and proper motion) generate two vector fields on the sphere. Fig. 3 shows the field of position differences, averaged on a suitable grid.

The analysis of vector fields on a sphere is better done using vector spherical harmonics (Mignard & Morando 1990). Let

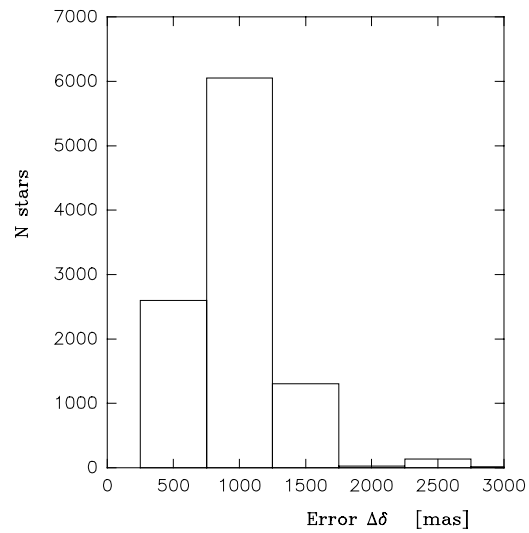
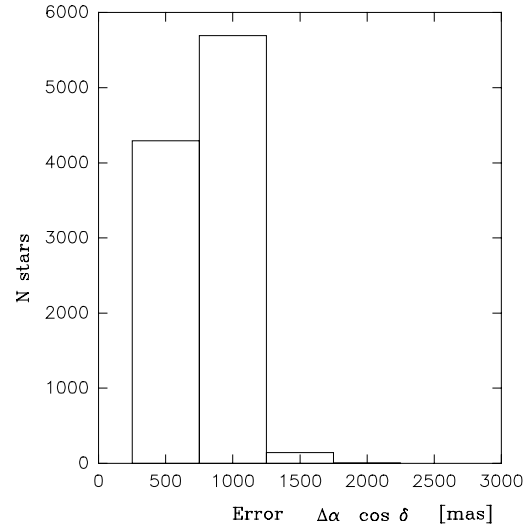


**Fig. 2.** Histogram of absolute values of errors in difference of position SAO-Hipparcos

$(\theta, \phi)$  be the spherical angular coordinates,  $Y_{lm}(\theta, \phi)$  the usual spherical harmonics and  $\mathbf{e}_\theta, \mathbf{e}_\phi$  the unit vectors in the  $\theta$  and  $\phi$  directions on the sphere. Then, two families of vector functions are defined through the equations:

$$\mathbf{T}_{lm}(\theta, \phi) = \frac{1}{\sqrt{l(l+1)}} \left[ -\frac{\partial Y_{lm}}{\partial \theta} \mathbf{e}_\phi + \frac{1}{\sin \theta} \frac{\partial Y_{lm}}{\partial \phi} \mathbf{e}_\theta \right] \quad (3)$$

$$\mathbf{S}_{lm}(\theta, \phi) = \frac{1}{\sqrt{l(l+1)}} \left[ \frac{\partial Y_{lm}}{\partial \theta} \mathbf{e}_\theta + \frac{1}{\sin \theta} \frac{\partial Y_{lm}}{\partial \phi} \mathbf{e}_\phi \right] \quad (4)$$

called *toroidal* and *spheroidal* vector harmonics. They form together a complete basis for vector functions on the sphere. They obey the symmetry properties:

$$\mathbf{T}_{l,-m} = (-1)^m \mathbf{T}_{lm}^* \quad (5)$$

$$\mathbf{S}_{l,-m} = (-1)^m \mathbf{S}_{lm}^* \quad (6)$$

and the orthogonality relations:

$$\int \mathbf{T}_{lm} \cdot \mathbf{T}_{l'm'}^* d\Omega = \delta_{ll'} \delta_{mm'} \quad (7)$$

$$\int \mathbf{S}_{lm} \cdot \mathbf{S}^*_{l'm'} d\Omega = \delta_{ll'} \delta_{mm'} \quad (8)$$

$$\mathbf{T}_{lm} \cdot \mathbf{S}_{lm} = 0 \quad (9)$$

Besides,  $\mathbf{T}$  is a solenoidal and  $\mathbf{S}$  an irrotational field:

$$\nabla \cdot \mathbf{T} = 0 \quad (10)$$

$$\nabla \times \mathbf{S} = 0 \quad (11)$$

Any square summable field  $\mathbf{V} = V_\theta \mathbf{e}_\theta + V_\phi \mathbf{e}_\phi$  on the sphere can be expanded in a Fourier series:

$$\mathbf{V}(\theta, \phi) = \sum_l \sum_{m=-l}^{m=l} [t_{lm} \mathbf{T}_{lm}(\theta, \phi) + s_{lm} \mathbf{S}_{lm}(\theta, \phi)] \quad (12)$$

whose complex Fourier coefficients are:

$$t_{lm} = \int \mathbf{T}_{lm}^* \cdot \mathbf{V} d\Omega \quad (13)$$

$$s_{lm} = \int \mathbf{S}_{lm}^* \cdot \mathbf{V} d\Omega \quad (14)$$

Our model assumes a finite Fourier expansion of real spherical vector fields. The reality conditions, together with the conjugation symmetry (5 y 6) imply that our model series has the form:

$$\mathbf{V} = \sum_{l=1}^{l_{\max}} [t_{l0}^{\Re} \mathbf{T}_{l0}^{\Re} + s_{l0}^{\Re} \mathbf{S}_{l0}^{\Re} + 2 \sum_{m=1}^l (t_{lm}^{\Re} \mathbf{T}_{lm}^{\Re} - t_{lm}^{\Im} \mathbf{T}_{lm}^{\Im} + s_{lm}^{\Re} \mathbf{S}_{lm}^{\Re} - s_{lm}^{\Im} \mathbf{S}_{lm}^{\Im})] \quad (15)$$

where the superscripts  $\Re, \Im$  denote the real and imaginary part of the function. The number of coefficients in the expansion is  $N_c = 2l(l+2)$ .

One of the nice properties of the vector harmonics expansion is that global effects between two catalogues are neatly packed in the  $l=1$  harmonics. Indeed, let  $\mathbf{A}$  be an infinitesimal rotation of the reference system. Then, it can be shown that the Cartesian components of the rotation vector are related to the  $l=1$  coefficients in the form:

$$A_1 = -\sqrt{\frac{3}{4\pi}} t_{11}^{\Re}, \quad A_2 = \sqrt{\frac{3}{4\pi}} t_{11}^{\Im}, \quad A_3 = \sqrt{\frac{3}{8\pi}} t_{10}^{\Re} \quad (16)$$

hereafter *rotation parameters*.

A global glide between the reference systems is defined through an irrotational vector  $\mathbf{G}$ , whose components are related to the  $s$  coefficients:

$$G_1 = -\sqrt{\frac{3}{4\pi}} s_{11}^{\Re}, \quad G_2 = \sqrt{\frac{3}{4\pi}} s_{11}^{\Im}, \quad G_3 = \sqrt{\frac{3}{8\pi}} s_{10}^{\Re} \quad (17)$$

hereafter *glide parameters*. This is important, since the main differences between both reference frames are global transformations.

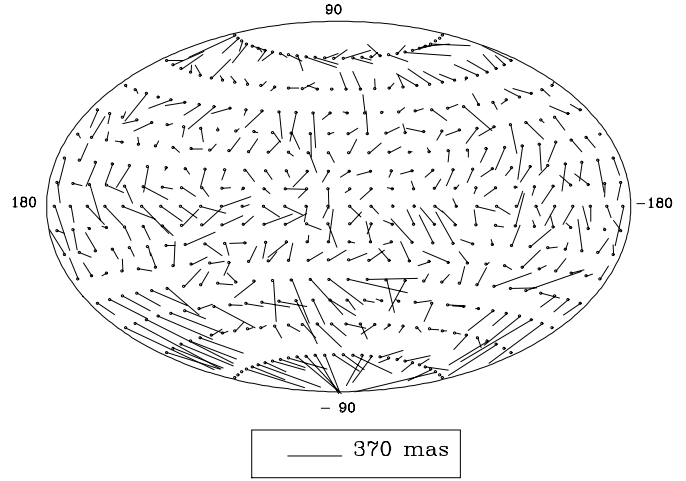


**Fig. 3.** SAO-Hipparcos position difference field, averaged on a  $12^\circ \times 12^\circ$  grid

## 9. The adjustment

The set of coefficients  $(t_{lm}, s_{lm})$  that define the model were found through least squares adjustment (Arley 1950, Bevington 1968). Each of the  $N_D$  data points provides us with two equations of condition; namely, the  $\alpha$  and  $\delta$  components of the spherical vector equation (15). The design matrix can be constructed straightforwardly, although its huge size ( $\sim 10000 \times 2950 \sim 100\text{Mb}$  for  $l=35$  and simple precision) made necessary a careful programming of the least squares routine.

The existence of large systematic errors in the SAO catalogue for polar stars suggested the introduction of a weighting scheme. For each difference  $\Delta$  in each observation  $i$  an effective standard deviation was introduced in the form:

$$\sigma_\Delta^2(i) = \sigma_{\Delta(SAO)}^2(i) + \sigma_{\Delta(Hipp)}^2(i) \quad (18)$$

and the weight factors were introduced as:

$$p_\Delta(i) = \frac{\sigma_\Delta^2(i)}{\sigma_\Delta^2(i)} \quad (19)$$

where the normalization factor  $\sigma_\Delta^2$  is:

$$\frac{1}{\sigma_\Delta^2} = \frac{1}{N_D} \sum_{i=1}^{N_D} \frac{1}{\sigma_\Delta^2(i)} \quad (20)$$

To simplify the construction of the weighted normal equations, each of the conditional equations was multiplied by the square root of the effective weight (19).

Another important parameter to adjust is the maximum degree of the Fourier series  $l_{\max}$ . This was done by a simple examination of the RMS of the adjustment:

$$\text{RMS}^2 = \frac{\frac{1}{\nu} \sum_{i=1}^{N_D} \frac{(O-C_i)^2}{\sigma_\Delta^2(i)}}{\frac{1}{N} \sum_{i=1}^{N_D} \frac{1}{\sigma_\Delta^2(i)}} \quad (21)$$

which is related to the  $\chi^2$  statistic through the equation:

$$\chi^2 = \nu \frac{\text{RMS}^2}{\sigma_\Delta^2} \quad (22)$$

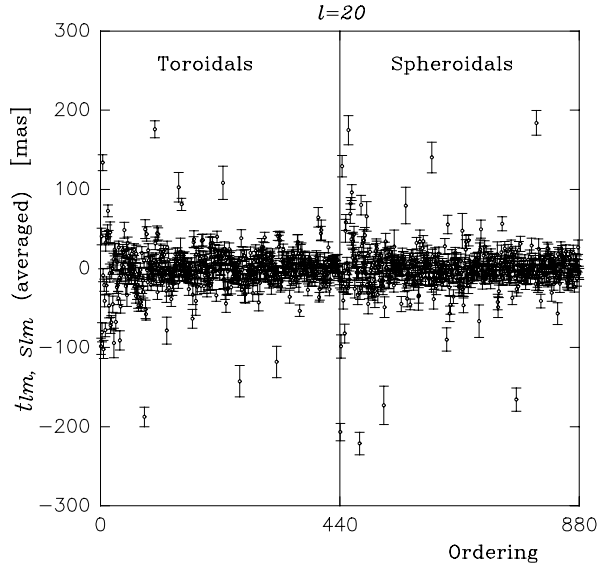


**Fig. 4.** Coefficients of the series representation of the positional differences, averaged over 10 groups for the final adjustment with  $l_{\max} = 20$ . The ordering indicates the position of the coefficients into the least squares equations, the first 440 represent the toroidals and the followings the spheroidals ones

and to the Birge ratio

$$R_B = \sqrt{\frac{\chi^2}{\nu}} \quad (23)$$

used in the least squares process as a scale factor of the uncertainties (Cohen & Taylor 1987).

For each of the groups of stars, several least squares adjustments were carried out varying the degree of the Fourier series  $l_{\max}$  from 1 to 20. It is found that the RMS stabilizes around  $RMS \sim 500$  mas for  $l_{\max} = 20$  in the case of positional parameters. On the other hand,  $l_{\max} = 10$  was enough to find stable values of the proper motion parameters.

As a final process, outliers were eliminated using the  $r$ -statistic of Arley (1950). These were defined as stars with reduced residuals (as defined in reference Arley (1950)) with  $r > 3$ . Several fits were carried with this process with  $l_{\max} = 10, 20$  and 35, eliminating as many outliers as found. The number of remaining stars in each group, as well as the final RMS and Birge ratio  $R_B^2$  are shown in Table 2.

## 10. Results and conclusions

Table 3 shows our results for the rotation parameters for several selected values of  $l_{\max}$ , averaged over the ten groups. The stated  $1\sigma$  errors reflect the dispersion between the different star groups. The corresponding results for the glide parameters are shown in Table 4. Table 5 shows the corresponding adjusted parameters for the proper motions. These latter parameters are much better behaved and an adjustment with  $l_{\max} = 10$  without outliers elimination was enough to represent the differences. Fig. 4 shows the coefficients of the adjusted series, averaged on the ten star groups. These are the main results of our analysis.

**Table 2.** Final statistics of the adjustment. The columns show the number of retained stars  $N_S$ , the RMS of the adjustment and the squared Birge ratio  $R_B$ . For the  $l = 35$  adjustment, the stars were eliminated with a previous  $l = 10$  adjustment

| Group | $l = 20$ |       |         | $l = 35$ |       |         |
|-------|----------|-------|---------|----------|-------|---------|
|       | $N_S$    | RMS   | $R_B^2$ | $N_S$    | RMS   | $R_B^2$ |
| G1    | 9482     | 494.6 | 2.71    | 9483     | 537.6 | 2.65    |
| G2    | 9471     | 518.4 | 2.66    | 9478     | 596.2 | 2.64    |
| G3    | 9441     | 511.4 | 2.70    | 9447     | 553.2 | 2.66    |
| G4    | 9462     | 510.6 | 2.66    | 9479     | 500.0 | 2.64    |
| G5    | 9471     | 512.5 | 2.60    | 9486     | 492.8 | 2.56    |
| G6    | 9404     | 564.6 | 2.62    | 9429     | 576.4 | 2.61    |
| G7    | 9470     | 551.8 | 2.60    | 9480     | 535.8 | 2.56    |
| G8    | 9443     | 536.8 | 2.67    | 9450     | 548.6 | 2.62    |
| G9    | 9472     | 530.4 | 2.72    | 9489     | 491.3 | 2.69    |
| G10   | 9477     | 485.0 | 2.63    | 9427     | 552.4 | 2.53    |

**Table 3.** Rotation parameters for several  $l_{\max}$ . MP are the values obtained with the soft used for check ours results

| Adj       | $A_1 \pm \sigma$ | $A_2 \pm \sigma$ | $A_3 \pm \sigma$ |
|-----------|------------------|------------------|------------------|
| $l5 - 20$ | $-14.3 \pm 1.7$  | $-21.3 \pm 1.8$  | $-33.3 \pm 3.0$  |
| $l10$     | $-16.6 \pm 6.0$  | $-30.7 \pm 5.4$  | $-17.5 \pm 3.0$  |
| $l20$     | $-19.7 \pm 5.1$  | $-39.4 \pm 6.0$  | $-34.0 \pm 3.5$  |
| $l35$     | $-23.7 \pm 5.4$  | $-41.2 \pm 5.0$  | $-40.4 \pm 4.5$  |
| MP        | $-37.0 \pm 5.7$  | $-55.5 \pm 5.7$  | $-59.0 \pm 5.7$  |

**Table 4.** Glide parameters for severals  $l_{\max}$  and for MP

| Adj       | $G_1 \pm \sigma$ | $G_2 \pm \sigma$ | $G_3 \pm \sigma$ |
|-----------|------------------|------------------|------------------|
| $l5 - 20$ | $39.3 \pm 1.7$   | $-5.5 \pm 1.2$   | $-70.4 \pm 1.3$  |
| $l10$     | $40.5 \pm 5.6$   | $-9.4 \pm 5.2$   | $-71.3 \pm 3.5$  |
| $l20$     | $48.2 \pm 7.2$   | $-7.7 \pm 5.4$   | $-71.5 \pm 3.8$  |
| $l35$     | $54.5 \pm 4.7$   | $-11.1 \pm 4.8$  | $-70.6 \pm 4.5$  |
| MP        | $66.4 \pm 8.3$   | $-22.1 \pm 7.0$  | $-87.6 \pm 5.7$  |

**Table 5.** Rotation and glide parameters for the proper motion difference field

| Adj       | $A_1 \pm \sigma$ | $A_2 \pm \sigma$ | $A_3 \pm \sigma$ |
|-----------|------------------|------------------|------------------|
| $l4 - 10$ | $0.04 \pm 0.03$  | $0.61 \pm 0.04$  | $0.62 \pm 0.05$  |
| Adj       | $G_1 \pm \sigma$ | $G_2 \pm \sigma$ | $G_3 \pm \sigma$ |
| $l4 - 10$ | $-0.01 \pm 0.03$ | $0.13 \pm 0.03$  | $-0.77 \pm 0.04$ |

Our analysis of the statistical properties of the series shows that  $l_{\max} = 20$  and  $l_{\max} = 10$  are enough to represent correctly the difference fields for position and proper motions. As a check, we compared the results with a vectorial analysis program by F. Mignard (Mignard 1999), named MP for us, which gives results similar to ours, with differences of about 10%. These differences are due to the different weighting schemes. The differences in proper motion are much smaller and do not show the presence of outliers.

Our results reveal the existence of several large distortions in the SAO reference system positions, evidenced by large Fourier coefficients of large order. The most important effects are in declination, associated with a large displacement field towards the South Pole (Fig. 3). Taking into account that the HIPPARCOS reference frame, being a materialization of the ICRS, is essentially free of these distortions, these zonal effects are due to the SAO catalogue errors. The present series may correct the main systematic effects.

*Acknowledgements.* The authors are very grateful to François Mignard for sharing his vectorial analysis of catalogues programs. E.F.A, R.B.O and H.V acknowledge partial support from FCAGLP and CONICET. R.B.O thank too the Instituto de Astrofísica de La Plata. R.G.C wishes to thank the FCAG for a student fellowship.

## References

- Andersen J. (ed.), 1999, Transactions of the IAU XXIII B. Dordrecht: Kluwer
- Arias E.F., Charlot P., Feissel M., Lestrade J.-F., 1995, A&A 303, 604
- Arley N., Buch P., 1950, Introduction to the theory of probability and statistics. New York: Wiley
- Bergeron J. (ed.), 1992, Transactions of the IAU XXIB. Dordrecht: Kluwer, p. 41
- Bevington P.R., 1968, Data reduction and error analysis for the physical sciences. New York: McGraw-Hill
- Cohen E.R., Taylor B.N., 1987, Rev. Mod. Phys. 59, 1121
- ESA, 1997, The Hipparcos and Tycho Catalogues, SP-1200
- Folkner W.M., Charlot P., Finger M.H., et al., 1994, A&A 287, 279
- Kovalevsky J., Lindegren L., Perryman M.A.C., et al., 1997, A&A 323, 620
- Ma C., Arias E.F., Eubanks T.M., et al., 1997, The international celestial reference frame realized by VLBI, in: Ma C., Feissel M. (eds.), IERS Technical Note 23, Observatoire de Paris
- Ma C., Arias E.F., Eubanks T.M., et al., 1998, AJ 116, 516
- Mignard F., Morando B., 1990, Analyse de catalogues stellaires au moyen d'harmoniques vectorielles, in: Capitane N., Débarbat S. (eds.), Colloque André Danjon, pp. 151–158
- Mignard F., 1999, private communication
- Mignard F., Froeschlé M., 2000, Global and local bias in the FK5 from Hipparcos data, A&A (in press)
- SAO Staff, 1966, Star Catalogue: Positions and proper motions of 258997 stars for epoch and equinox of 1950.0, Publ. Smithsonian Inst. of Washington D.C. 4562
- Roman N.G., Warren Jr W.R., 1990, The Smithsonian Astrophysical Observatory Star Catalogue, Documentation for the Machine-Readable Version